Published in final edited form as:

Brain Imaging Behav. 2017 August ; 11(4): 1071–1084. doi:10.1007/s11682-016-9572-z.

Disrupted functional connectome in antisocial personality disorder

Weixiong Jiang[1,2,3,4], **Feng Shi**[3], **Jian Liao**[1], **Huasheng Liu**[1], **Tao Wang**[3,5], **Celina Shen**[3], **Hui Shen**[4], **Dewen Hu**[4], **Wei Wang**[1], and **Dinggang Shen**[3,6]

[1]Department of Radiology, The Third Xiangya Hospital, Central South University, Changsha, Hunan 410013, China

[2]Department of Information Science and Engineering, Hunan First Normal University, Changsha, Hunan 410205, China

[3]Department of Radiology and BRIC, University of North Carolina at Chapel Hill, 130 Mason Farm Road, Chapel Hill, NC 27599-7513, USA

[4]College of Mechatronics and Automation, National University of Defense Technology, Changsha, Hunan 410073, China

[5]Shanghai Mental Health Center, Shanghai Jiao Tong University School of Medicine, Shanghai, China

[6]Department of Brain and Cognitive Engineering, Korea University, Seoul, Republic of Korea

Abstract

Studies on antisocial personality disorder (ASPD) subjects focus on brain functional alterations in relation to antisocial behaviors. Neuroimaging research has identified a number of focal brain regions with abnormal structures or functions in ASPD. However, little is known about the connections among brain regions in terms of inter-regional whole-brain networks in ASPD patients, as well as possible alterations of brain functional topological organization. In this study, we employ resting-state functional magnetic resonance imaging (R-fMRI) to examine functional connectome of 32 ASPD patients and 35 normal controls by using a variety of network properties, including small-worldness, modularity, and connectivity. The small-world analysis reveals that ASPD patients have increased path length and decreased network efficiency, which implies a reduced ability of global integration of whole-brain functions. Modularity analysis suggests ASPD patients have decreased overall modularity, merged network modules, and reduced intra- and inter-module connectivities related to frontal regions. Also, network-based statistics show that an internal sub-network, composed of 16 nodes and 16 edges, is significantly affected in ASPD patients, where brain regions are mostly located in the fronto-parietal control network. These results suggest that ASPD is associated with both reduced brain integration and segregation in

Correspondence to: Wei Wang; Dinggang Shen.

Weixiong Jiang and Feng Shi are co-first authors.

Disclosures

All authors declare that they have no conflict of interest. All procedures followed are in accordance with the ethical standards of the responsible committee on human experimentation (institutional and national) and with the Helsinki Declaration of 1975, and the applicable revisions at the time of the investigation. Written informed consent was obtained from all patients included in the study.

topological organization of functional brain networks, particularly in the fronto-parietal control network. These disruptions may contribute to disturbances in behavior and cognition in patients with ASPD. Our findings may provide insights into a deeper understanding of functional brain networks of ASPD.

Keywords

Antisocial personality disorder; Brain connectome; Topological organization; Modularity; Functional connectivity

Introduction

Antisocial personality disorder (ASPD) is one of the six personality disorders stated in the Diagnostic and Statistical Manual of Mental Disorders, Fifth Edition (DSM-V). The essential features of ASPD in dimensional model are antagonism and disinhibition, which are commonly linked to criminal behavior. It was reported that 47 % of male prisoners had been previously diagnosed with ASPD, according to a large-scale meta-analytic review in worldwide prison systems (Fazel and Danesh 2002). Moffitt et al. found most violent crimes were committed by a small number of men with ASPD (Moffitt et al. 2002). According to the criteria of DSM-V, men with ASPD display patterns of antisocial and aggressive behaviors that begin during childhood and remain stable throughout life. Lifelong patterns of poor self-control ability, impulsivity, and risk-taking behaviors are prevalent in those suffering from ASPD.

Morphological MRI studies found multiple brain structures that differed in ASPD groups. For example, Raine et al. found that the prefrontal gray matter volume in ASPD was reduced by about 11 %, as opposed to that of the control group (Raine et al. 2000). The reduced volume in the prefrontal cortex was replicated in many other studies of ASPD (Yang and Raine 2009). Violent individuals diagnosed with ASPD suffered from significant losses in anterior cingulate volume (Kumari et al. 2014). Sundram et al. showed that white matter fractional anisotropy (FA) decreased in the right frontal lobe in ASPD young males, indicating white matter microstructural abnormalities in the frontal lobe (Sundram et al. 2012). Meanwhile, functional MRI studies also found abnormal brain regions in ASPD. For example, autonomic activity in prefrontal gray matter was reportedly reduced in the galvanic skin response, as opposed to that of the control group (Raine et al. 2000). Schneider et al. unexpectedly found increased emotional response of ASPD in the amygdala and dorsolateral prefrontal cortex (Schneider et al. 2000). By using amplitude of low-frequency fluctuations (ALFF) and regional homogeneity (ReHo), studies also found that ASPD patients showed decreased activities in the fronto-temporal brain regions during resting states (Liu et al. 2014; Tang et al. 2013). However, previous studies on ASPD mainly focused on abnormalities of individual brain regions. As is known, the human brain is a complex interconnected network with powerful functionality of both functional segregation and functional integration.

Numerous research studies have suggested that human whole-brain networks, including structural and functional networks, can be characterized quantitatively using topological

properties based on the graph theory (Wee et al. 2014; Wang et al. 2013; Sporns 2011). Graph theory analyses can provide concise measures of the integration and segregation of interconnected networks (Rubinov and Sporns 2010). With topological metrics, many organizational principles, including small-worldness and modularity, have been observed in the human brain connectome. A small-world network can be characterized by high local specialization and high global integration between network nodes (Stam 2004; Latora and Marchiori 2003). Network modularity provides information about the extent of decomposability of a network by identifying modules of densely interconnected nodes, but sparsely connected across different modules (Newman 2006). Small-worldness and modularity provide rich quantitative insights into the organization of complex brain networks (Shi et al. 2012). In fact, these network properties have been found disrupted in patients with various neuropsychiatric disorders (Wee et al. 2014; Peng et al. 2014; Shi et al. 2012; Zhang et al. 2011). Specially, psychopathy patients were lately found with reductions in small-world network properties, which indicate an integrative deficit (Philippi et al. 2015). As generally known, psychopathy has multiple overlaps with ASPD in diagnostic criteria. Recent researches have also observed changes to modular structure of functional networks in diverse pathological conditions (Gamboa et al. 2014; Arnemann et al. 2015; Vaessen et al. 2013). For psychopathy, the network modularity seems less coordinated due to the lack of connections between distant hubs (Philippi et al. 2015). Graph theoretical approaches have been shown as a promising tool to characterize pathological conditions; however, to our knowledge, there is no report of the graph theory study of ASPD. Thus, the topological organization of whole-brain functional networks in ASPD still remains poorly understood.

In this study, we utilized resting-state functional magnetic resonance imaging (R-fMRI) to investigate the topological architecture of intrinsic brain networks in patients with ASPD. R-fMRI has been extensively used to reveal functional abnormalities of the brain (Peng et al. 2014; Shi et al. 2012; Wang et al. 2013). We hypothesize that ASPD disrupts the topological organization of intrinsic functional connectome, and thus leads to reduced functional integration. To test this hypothesis, we collected R-fMRI data from 32 ASPD patients and 35 healthy control subjects, and analyzed their between-group differences of intrinsic functional connectome using graph theoretical approaches. We also determined the possible functional connectivity changes by using network-based statistics (NBS).

Methods and materials

Participants

All volunteers were recruited from the School for Youth Offender of Hunan Province, where they received reformatory education as a result of certain crimes, e.g., robbery and violent attacks. “Enclosed-style” management and regular school hours were implemented daily in this school. All young offenders were of legal age (age > 18 years) to give consents to participate in the experiments, but were under the legal age when they had originally entered the school. All volunteers were first tested in groups at the school using the Personality Diagnostic Questionaire-4+ (PDQ-4+) by a professional with experience in psychological testing. The subjects with ASPD scores equal to or above 4 score were continuously tested

by two senior psychiatrists to determine whether they had Axis 1 disorders of major mental illness. Those with Axis 1 disorder were excluded. The rest subjects were tested using the Personality Disorder Interview (PDI-IV) for personality disorders. Note that PDI-IV is a semi-structured interview that yields a rating for each of the DSM-IV personality disorders (Widiger and Costa 1994). In this step, subjects were excluded if they were accompanied with any other personality disorders. Finally, 32 subjects diagnosed only with ASPD were found to comply with criteria and included in this study. All ASPD disorders met both PDQ-4 criteria and PDI-IV criteria for ASPD. In the meantime, we also chose 35 controls subjects who *neither* met PDQ-4 criteria *nor* met PDI-IV criteria for ASPD. All the controls were tested using the same above methods. All subjects had normal IQ when tested using the Wechsler Adult Intelligence Scale. The control subjects without ASPD were matched to the ASPD subjects in age, education, and IQ using One-way ANOVAs (Table 1).

All subjects were right-handed, native Chinese speakers. They had no access to alcohol for at least 6 months prior to the brain scan. They had no history of substance abuse or any major head trauma, as well as history or current diagnosis of serious mental disorders, e.g., anxiety neurosis, depression or schizophrenia. Three teachers accompanied each participant while undergoing the fMRI scans.

Data acquisition and preprocessing

All subjects underwent a resting-state fMRI using a 1.5 T Siemens Trio scanner, with an 8-channel phased array head coil, at the Third Xiangya Hospital of Central South University. During the scan, subjects were instructed to relax, close their eyes, remain awake, and perform no specific cognitive exercise. These conditions were later confirmed with a survey that included whether they fell asleep and what they were thinking during the scanning process. Magnetic resonance imaging (MRI) scans were performed using a gradient-echo EPI sequence, and the imaging parameters were as follows: TR = 2000 ms, TE = 50 ms, FA = 90°, matrix = 64 × 64, slices = 23, FOV = 240 mm ×240 mm, and resolution = 3.75 × 3.75 × 5 mm^3. Every resting-state functional session lasted 5 min, and totally 150 volumes were obtained.

The R-fMRI images were processed using DPARSF (Yan and Zang 2010). Specifically, for each subject, the first 5 volumes of the scanned data were removed due to magnetic saturation. The remaining 145 volumes were corrected through registering and re-slicing to control for head motion. All subjects in this study had no more than 1 mm translation in the x, y, or z-axes and less than 1 degree of rotation in each axis. Next, the volumes were normalized to the standard EPI template in the Montreal Neurological Institute (MNI) space and resampled into 3 mm isotropic voxels. Then, smoothing and filtering were performed using a Gaussian filter of 8 mm full-width half-maximum kernel and a Chebyshev band-pass filter (0.01–0.08 Hz), respectively. Finally, several nuisance covariates, including head motion parameter, white matter signals, and cerebrospinal fluid signals, were regressed from the image to remove some potential sources of physiological noise in functional connectivity analysis (Biswal et al. 2010; Dosenbach et al. 2010). Considering the controversy of removing the global signal when preprocessing RS-fMRI data (Fox et al. 2009; Murphy et

al. 2009), we did not include the global signal in our regression process (Lynall et al. 2010; Wang et al. 2013; Supekar et al. 2008).

Construction of brain functional network

Brain networks were constructed at macro-scale, where nodes represented brain regions and edges represented interregional functional connectivity. In order to define the nodes, we parcellated the entire brain into 90 brain regions of interest (ROIs) (45 ROIs per hemisphere) according to the anatomical automatic labeling atlas (AAL) (Tzourio-Mazoyer et al. 2002). Regional mean time series were obtained for each subject by averaging the fMRI time series over all the voxels in each of the 90 regions. Then, the network edges were defined as interregional resting-state functional connectivity, obtained by computing Pearson's linear correlation coefficient between the mean time series of each pair of the regions. For each subject, we obtained a resting-state functional network that was expressed as a 90 × 90 symmetrical matrix.

As of now, most brain network studies used binarized graphs to investigate the brain's topological properties (Zhang et al. 2011; Peng et al. 2014; Shi et al. 2012). These methods require thresholds for each correlation matrix repeatedly over a wide range of sparse levels, and obtain different results for different thresholds. In this study, we used weighted network, i.e., the raw correlation coefficient matrix, to study network attributes that take into account the network edge strength in terms of functional connectivity. Thus, the weighted network may be able to demonstrate more natural representations of the brain organization. We employed network analysis for ASPD at three levels, i.e., global small-worldness, modularity, and connectivity.

Global small-world measure

Small-world properties for a weighted network were characterized by the clustering coefficient C^w and the shortest path length L^w (Watts and Strogatz 1998; Wang et al. 2013), which quantify efficiency of information transfer of a network at both local and global levels. Their normalized versions $(\tilde{C}^w, \tilde{L}^w)$ were obtained using random networks. A small-world network typically shows $\tilde{C}^w > 1$ and $\tilde{L}^w \approx 1$ (Watts and Strogatz 1998). Details of mathematical definitions could be found in Appendix.

Besides the conventional small-world parameters $(\tilde{C}^w \& \tilde{L}^w)$, network efficiency metrics were also used to provide more biologically sensible properties for brain networks. Specifically, the global efficiency (E^w_{glob}) and local efficiency (E^w_{loc}) quantify the extent of information transmission at the global network and the individual node levels, respectively (Latora and Marchiori 2001). Details of their mathematical calculations can be found in Appendix.

Modular analysis

Modularity is an important organizational principle for brain networks (Meunier et al. 2010). Brain network is comprised of multiple modules by functional specialization and integration (Rubinov et al. 2009). A complex network can be partitioned into modules using a modified

greedy optimization algorithm by searching for the partition that maximizes the number of connections within modules, and also minimizes the number of connections between modules (Newman and Girvan 2004; Reichardt and Bornholdt 2006). To assess the extent of modular organization, i.e., the degree to which a graph can be divided into non-overlapping modules, weighted modularity metric Q^w was calculated for the individual network (Shi et al. 2013). To assess the inter- and intra-modular connectivities, the sum of all connectional weights within one module was defined as an index of intra-module connectivity, and the total connectional weights between two modules can be used as an index of inter-module connectivity (Guimera and Amaral 2005).

Based on the modules identified by Newman's algorithm (Newman and Girvan 2004), we also calculated the participation coefficient (PC) and intra-module degree (MD) for each node. Participation coefficient was a measure of a node's importance in inter-modular communication, while intra-module degree was a measure of a node's importance in intra-modular communication. Details of mathematical definitions were listed in Appendix. The Brain Connectivity Toolbox (http://www.brainconnectivity-toolbox.net) was used in this paper for the network measure computation.

Functional connectivity analysis

To identify the functional connectivity that was altered in ASPD patients, a network-based statistic (NBS) approach was used (Zalesky and Fornito 2010). In brief, a primary cluster-defining threshold ($t = 3$, $p = 0.05$) was first used in the t-statistic (two-sample one-tailed t-tests) that was computed for each connection, so as to identify supra-threshold connections within which any connected components and their number were then determined. Next, the null distribution of connected component size was empirically derived using a nonparametric permutation approach (5000 permutations) to estimate the significance for each component. A corrected p value was determined for each component using the null distribution of maximal connected component size. The same primary threshold ($t = 3$) was used to generate supra-threshold links, among which the maximal connected component size was recorded. Finally, a connected component of size M can be found between controls and patients, i.e., those components show significant changes in ASPD patients in comparison to that of controls. Notably, the effects of age, education, and IQ were removed by a regression analysis prior to the statistical analysis of functional connections. The details of network-based statistical analyses can be found in (Zalesky and Fornito 2010).

Statistical analysis

To determine group differences in small-world and modular measures, nonparametric permutation tests were performed on each metric, and corresponding p values were then reported (Bullmore et al. 1999; Zhang et al. 2011). In brief, we initially calculated the between-group difference of the mean values for each small-world or modular metric. To test the null hypothesis that the observed group differences only occurred by chance, each small-world or modular metric value was randomly reallocated into two groups (10,000 permutations), and then the mean difference between two randomized groups was recomputed. The 95th percentile points of each distribution were used as critical values for a one-tailed test to determine whether the observed group differences could occur by chance.

Before the permutation tests, multiple linear regression analyses were applied to remove confounding effects of age, education, and IQ for each network metric. Note that gender was not included, as all participants were males.

Results

Abnormalities of small-world properties in ASPD patients

The weighted network of both ASPD and HC groups exhibited typical features of small-world topology, i.e., higher clustering coefficients but almost identical characteristic path lengths, compared to matched random networks.

Nevertheless, quantitative statistical analyses revealed significant differences in both small-world parameters and network efficiency between ASPD patients and control subjects (Fig. 1). The ASPD group showed significantly higher values in both characteristic path length ($p = 0.0204$) and normalized characteristic path length ($p = 0.0204$), compared to the values of normal control subjects. No significant differences were found in clustering coefficients ($p = 0.1146$). As for network efficiency, comparisons revealed both decreased global efficiency ($p = 0.0385$) and local efficiency ($p = 0.0299$) in the ASPD group.

Modularity differences in ASPD patients

Modular organizations—Four functionally oriented modules were detected in the HC group, but only three modules in the ASPD group. The surface representations for functional modules are shown in Fig. 2. Below are the four modules in the HC group.

- *Posterior (Module I)*: Comprising occipital regions in the primary visual cortex and their adjacent areas. ASPD patients were almost the same as the control subjects in this module, except one additional brain region, i.e., right inferior temporal gyrus (ITG).
- *Central (Module II)*: Including motor, somatosensory, and superior temporal regions (auditory system), as well as the bilateral insula. ASPD patents were also similar to the control subjects in this module, except for four additional brain regions, i.e., bilateral hippocampus (HIP) and parahippocampal gyrus (PHG).
- *Frontal-Subcortical (Module III)*: Mostly involved in apathy and disinhibition (Bonelli and Cummings 2007), including medial frontal cortex, part of the orbitofrontal cortex, subcortical structures, and middle temporal gyrus. For the ASPD group, this module did not appear independently.
- *Frontoparietal (Module IV)*: Including frontal, inferior parietal, angular, and inferior temporal regions in the healthy group, which are mainly associated with cognition control function (Cole et al. 2014). In ASPD group, this module also did not appear independently.

Modules I and II in the HC group are mostly similar to those in the ASPD group. Interestingly, Modules III and IV in the HC group are merged into a single Module III in the ASPD group.

Quantitative statistical analyses revealed significant difference in the global brain modularity between ASPD patients and control subjects ($p = 0.0268$).

Alterations in the intra- and inter-module connectivity—To compare functional modules between the groups, the mean modular organization in healthy controls was used as a more optimized functional organization. The mean functional modules in healthy controls were then applied to all subjects' brain networks to evaluate the intra-module connectivity and inter-module connectivity. Our results found that ASPD patients showed significantly reduced modularity in frontal-subcortical module ($p = 0.0268$) and frontoparietal module ($p = 0.001$), compared to the healthy controls (Fig. 3a).

We then examined inter-module connectivity between groups using the four functional modules obtained from healthy controls. Compared with healthy controls, ASPD patients showed significantly decreased inter-module connectivity between frontal-subcortical and frontoparietal modules ($p = 0.0121$) (Fig. 3b).

Regional roles of module connectivity—Participation coefficient measures a node's importance in inter-modular communication. For the participation coefficient of each node, nonparametric permutation tests revealed significant differences mainly in the prefrontal and parietal regions, as well as left posterior cingulate gyrus and superior temporal gyrus (Table 2). Aside from the left posterior cingulate gyrus, the participation coefficient values of the above brain regions all decreased.

Intra-module degree measures a node's importance in intra-modular communication. For the intra-module degree of each node, nonparametric permutation tests revealed significant differences mainly in the prefrontal and temporal regions with decreased intra-module degree, and the posterior cingulate gyrus, but with increased intra-module degree (Table 2).

Functional connectivity alterations in ASPD patients

We utilized the NBS method and identified a single connected sub-network with 16 nodes and 16 connections that showed significant differences between ASPD patients and control subjects (Fig. 4). Within this sub-network, all connections exhibited decreased values in ASPD patients, compared to those of control subjects. Among the 16 connections, 6 connections were located between frontal and parietal gyri, and 8 connections located between frontal or parietal gyrus and other gyrus, including 3 connections between fusiform and supramarginal gyri (a portion of the parietal lobe). We can observe that the disturbed connections are mostly related to fronto-parietal control network.

Discussion

The present study examined functional brain networks in ASPD patients for small-world, modularity, and connectivity properties. The small-world analysis reveals that ASPD patients have increased path length and decreased network efficiency, implying a reduction of normal global integration of whole-brain networks. Modularity analysis suggests that ASPD patients have decreased modularity and different network modular organizations from control group. NBS analysis shows that an internal sub-network, composed of 16 nodes and

16 edges, is significantly affected in ASPD patients, where the brain regions are located mostly in the fronto-parietal control network. All results suggest that ASPD is associated with disruptions in topological organization of functional brain networks.

Abnormalities of small-world property in ASPD patients

Small-worldness enables high efficiency of both specialized and integrated processing within a network (Watts and Strogatz 1998; Latora and Marchiori 2003; Wang et al. 2013). In this study, small-worldness was found in both ASPD and control groups, suggesting an optimal organization of the human brain to support efficient information communication. However, quantitative analysis revealed significant group differences in both characteristic path length and network efficiency. Specifically, the ASPD patients showed increased path length and decreased local efficiency and global efficiency, compared to the control subjects, which indicates a disturbance of global integration of whole-brain networks in ASPD patients. In parallel to the increase in characteristic path length, the average physical connection distance also decreased in ASPD, which suggests a loss of connections between certain remote brain regions. Long-range connections are believed to underlie cognitive processing through effective integrity and rapid information propagation between and across remote regions of the brain (Sporns and Zwi 2004), as increased path length in ASPD suggests difficulty in certain cognitive processing. Network efficiency describes brain networks from parallel information flow, which is a more biologically relevant measure (Latora and Marchiori 2001). On the other hand, global efficiency measures the ability of parallel information transmission throughout the brain network. Local efficiency measures the fault tolerance of the network, indicating the capability of information communication for each subgraph when the central node is eliminated. Both global and local efficiencies decreased in ASPD, implying disruption of brain network in ASPD patients. The changes in these global network metrics may be attributed to decreased functional connections in ASPD patients, mainly those related to fronto-parietal control network. The decreased small-world properties have been found in a number of brain disorders, e.g., depressive disorder (Zhang et al. 2011), Alzheimer’s disease (Wang et al. 2013), and schizophrenia (Shi et al. 2012).

Modular organization differences in ASPD patients

Modularity enables faster adaptation by changing functionality of one module without losing functionality in other modules. Random networks have less modularized information processing or fault tolerance, compared with small-world networks (Latora and Marchiori 2001). In this study, small-worldness and modularity were found in both ASPD and control groups. This suggests the optimal organization of the human brain to support efficient information transfer of both modular and distributed processing (Wang et al. 2013). Our results on modular architecture of the resting-state functional networks of the control groups are generally in accordance to previously reported modular decompositions of the resting-state correlation networks (Balenzuela et al. 2010; Tagliazucchi et al. 2013; Gamboa et al. 2014), with modules parallel with well-defined brain systems (i.e., visual areas, frontoparietal network, central sensory-motor module, etc.). These results provide confidence on the modularity decomposition as a method to quantify global brain interactions. Quantitative statistical analyses revealed decreased modularity in ASPD patients. Furthermore, ASPD patients showed decreases in intra-modularity for both frontal-

subcortical and fronto-parietal modules. They also showed decreased inter-module connectivity between frontal-subcortical and fronto-parietal modules, compared to healthy controls. A decrease in the local/global efficiency in small-worldness was a reflection of the intra−/inter-module connectivity. Based on these outcomes, there is an obvious ASPD abnormality present. In our study, regions in frontal-subcortical module were mostly involved in apathy and disinhibition (Bonelli and Cummings 2007). The anterior cingulate circuit, including the medial frontal cortex, anterior cingulate, and pallidus, is related to emotional information integration; and the orbitofrontal circuit, including the orbitofrontal cortex and caudate, allowed the inhibition of behavioral responses. Fronto-parietal module is mainly associated with cognition control function (Cole et al. 2014). The decrease of connectivity in and between these modules may result in deficits in cognitive, behavioral control, and mood processing; thus, leading to poor self-control ability, apathy, impulsivity and risk-taking behaviors.

Less small-world characteristics and less modularity in ASPD patients may reflect a less optimal topological organization in brain connectome, which provides evidence that ASPD is a disorder with disrupted neuronal network organization.

Functional connectivity alterations in ASPD patients

Using network-based statistics, we identified a single network with weaker connections in the ASPD patients. These fewer connections during resting states may reflect essential disconnections of spontaneous neural activity. Disconnected connectivities were located mostly between frontal and parietal gyri, or between these two gyri and other brain regions, which indicates disturbances in the fronto-parietal control network in ASPD patients. These connections were directly related to whole-brain network topology, suggesting their contribution to observed global topological abnormalities. It is reasonable to speculate that these disconnections had led to decreased functional integration throughout the brain, which may further account for cognitive deficits in ASPD patients. The fronto-parietal control system plays an important role in maintenance and improvement of mental health, as an intact control system is protective against a variety of mental illnesses (Cole et al. 2014). Fewer connections of the control system in ASPD may disturb its ability to regulate symptoms. The cortical regions in the fronto-parietal control system are highly interconnected (Power et al. 2011; Vincent et al. 2008), and have extensive brain-wide connectivity that allows for communicate with various systems throughout the brain (Power et al. 2011). Executive function reflects the higher order cognitive control of thought, action, and emotions. A study looking at damages to the prefrontal cortex in rhesus monkeys showed impairments in executive function, i.e. they had difficulties in establishing certain specific response pattern and then maintaining or shifting response patterns to other tasks (Moore et al. 2009). Neuropsychological deficits in executive function were thought to contribute to severe antisocial and aggressive behavior (Ogilvie et al. 2011; Raine et al. 2005; Seguin et al. 2007). Our finding about fewer connections in ASPD patients could further support this hypothesis and explain the cause for severe antisocial and aggressive behaviors from brain networks.

Brain region disruptions in ASPD patients

Combining modularity analysis and NBS analysis, we easily found consistent disruptions in brain regions, such as in the superior frontal gyrus (medial) (SFGmed), orbitofrontal cortex (OFC), posterior cingulate gyrus (PCG), superior parietal gyrus (SPG), inferior parietal lobule (IPL), and temporal pole (TPO). Many previous studies also found that individuals with antisocial personality disorder had reduced functioning in the prefrontal cortex (Yang and Raine 2009). Note that the medial frontal gyrus is closely related with high-level executive functions and decision-related processes (Talati and Hirsch 2005), and is also associated with a number of cognitive functions, which prevents specific performances, such as sustained attention (Demeter et al. 2011), and uncertainty (Volz et al. 2004a, 2004b). Risk-taking and impulsivity in ASPD may be related to poor decision-making caused by disruptions to the medial frontal gyrus.

Orbitofrontal cortex (OFC) is widely believed to be critical for flexible decision-making when the established choice values change. The medial OFC is involved in making stimulus-reward associations and in reinforcement of behavior, while the lateral OFC is involved in stimulus-outcome associations and in evaluation of behavior (Walton et al. 2010). Encoding new expectations about punishment and social reprisal is related to lateral OFC (Campbell-Meiklejohn et al. 2012; Meshi et al. 2012). The lateral OFC plays an important role in conflict resolution, and damages to this area can result in both inappropriate displays of anger and inappropriate responses to the anger of others (Meyers et al. 1992). Disruption of activity in this area, using transcranial magnetic stimulation or direct current stimulation, leads to changes in risk attitudes (Fecteau et al. 2007). Destruction of the OFC, through acquired brain injury, typically leads to patterns of disinhibited behavior-impulsivity, which is a core characteristic of ASPD. These converging lines of evidence suggest that, if the OFC cannot function properly, a person may act impulsively and inappropriately, and then produce antisocial emotions. The associated inability to act in a “civilized” manner often results in criminality.

The posterior cingulate is reported to be essential for conscious awareness (Vogt and Laureys 2005), and be involved in a range of cognitive tasks about self-processing (Cavanna and Trimble 2006; Buckner and Carroll 2007). The superior parietal cortex is critically important for manipulation of information in working memory (Koenigs et al. 2009), and in rule-based visual-motor transformations (Hawkins et al. 2012). The inferior parietal lobule is involved in perception of emotions in facial stimuli (Radua et al. 2010) and plays a key role in various cognitive functions, including attention, language, and action processing (Caspers et al. 2012). The right functions of the above regions are important for selection and control of socially relevant behavior.

The temporal lobe is involved in language comprehension and emotion association (Arfken 2009), whereas the temporal pole is associated with cognitive perspective taking (Meyer et al. 2013). Prior studies revealed that the right temporal pole plays a critical role in emotional empathy, both in emotional contagion and affective perspective-taking (Rascovsky et al. 2011; Zahn et al. 2009). The impairment in emotional comprehension and contagion may introduce changes in conduct and social behavior (Rascovsky et al. 2011; Zahn et al. 2009). Jastorff et al. found that the main cognitive component underlying middle temporal gyrus

activation in their study was the evaluation of action rationality (Jastorff et al. 2011). The temporal lobes take part in sensory, affective, and higher cognitive processing (Kolb and Whishaw 1990). The disruption of these areas found in these studies may be related with changes in conduct and social behavior in those with ASPD, thus resulting in violent, aggressive behaviors, or in development of affective instability, which are both core diagnostic criteria for ASPD.

In this study, the brain abnormality of ASPD appear in both temporal and frontal lobes, which is consistent with prior studies in aggression-prone individuals (Sundram et al. 2012; Wolf et al. 2015; Hoppenbrouwers et al. 2013). Certain types of antisocial activities are closely linked with frontal-temporal dysfunction, with joint abnormalities of the two regions predisposing some patients to antisocial behaviors (Miller et al. 1997). Compared to either area, independently, temporal and frontal lobe neuropathology co-occurring may increase the risk of anger and aggression (Potegal 2012). Neuropathology occurring in both areas has also been found in psychopathy, which is a similar disorder to ASPD and has many overlaps in diagnostic criteria. Psychopaths illustrate reduced gray matter volume both in the frontal and temporal regions, compared to gray matter volumes in the controls (de Oliveira-Souza et al. 2008; Muller et al. 2008a). Furthermore, an impaired emotion-cognition interaction in psychopaths is involved in changed prefrontal and temporal brain activation (Muller et al. 2008b). As a result of these findings, some studies have put forward theories that fronto-temporal brain abnormalities are associated with antisocial behavior disorders (Blair and Mitchell 2009), which were verified continuously (Sundram et al. 2012; Wolf et al. 2015; Hoppenbrouwers et al. 2013).

Conclusion

Overall, our results provide empirical evidence for disrupted network organization in ASPD patients at three (global, modularity, and connectional) levels for the very first time. These results suggest that ASPD is associated with disruptions in topological organization of functional brain networks, wherein these disruptions may contribute to behavioral and cognitive disturbances in ASPD patients. Our results provide insights for understanding the functional brain networks of ASPD. As of now, some researchers have already started examining ways to reduce the clinical severity of ASPD through medicinal interventions and selective treatment (Brown et al. 2014). Our results may provide some useful information for their further consideration.

Acknowledgments

We thank all the volunteers for their participation in the study and the anonymous referees for their insightful comments and suggestions. The Funding Project of Education Ministry for the Development of Liberal Arts and Social Sciences (13YJCZH068), the China Postdoctoral Science Foundation (2015 M582879) and Key Laboratory of Basic Education Information Technology of Hunan Province (2015TP1017) helped support this work. Additionally, this study was partially supported by the National Natural Science Foundation of China (61420106001, 61375111, 81571298) and, in part, supported by NIH grants (AG041721, EB006733, EB008374, EB009634).

Appendix

Small-world Analysis

The small-world architectures of a network could be obtained by calculating clustering coefficient and characteristic path length (Watts and Strogatz 1998). For a weighted network *N* the clustering coefficient C^w is the average of all nodal clustering coefficients, where nodal clustering coefficient C_i^w for a given node *i* is defined as (Onnela et al. 2005):

$$C_i^w = \frac{1}{n}\sum_{i\in N}\frac{\sum_{j,h\in N}\left(w_{ij}w_{ih}w_{jh}\right)^{1/3}}{k_i\left(k_i-1\right)} \quad (1)$$

Where *n* is the number of nodes, k_i is the degree of node *i*, i.e., the number of non-zero connections, w_{ij} is connection weights between node *i* and node *j*. The clustering coefficient quantifies the extent of local interconnectivity or cliquishness of a network. The characteristic path length L^w of a weighted network *N* with *n* nodes is defined as:

$$L^w = \frac{1}{n}\sum_{i\in N}\frac{\sum_{j\in N, j\neq i} d_{ij}^w}{n-1} \quad (2)$$

where d_{ij}^w is the weighted shortest path length between node *I* and node *j* and is computed as the smallest sum of the edge lengths throughout all of the possible paths in the network from node *i* and node *j*. The characteristic path length reflects the mean distance or routing efficiency between any given pair of nodes.

Their normalized versions $(\tilde{\mathrm{C}}^{\mathrm{W}}, \tilde{\mathrm{L}}^{\mathrm{W}})$ were obtained using random networks, i.e., dividing the real values C^w and L^{W} by the corresponding mean derived from 100 random networks that preserved the same number of nodes, edges and degree distributions as the real brain networks (Maslov and Sneppen 2002; Sporns and Zwi 2004). During the random rewiring procedure, we specially retained the weight of each edge. A small-world network typically shows $\tilde{C}^w > 1$ and $\tilde{L}^w \approx 1$ (Watts and Strogatz 1998).

Network Efficiency

Network efficiency metrics can be used to provide more biologically sensible properties for brain networks. The global efficiency (E_{glob}^w) and local efficiency (E_{loc}^w) quantify the extent of information transmission at the global network and the individual node levels, respectively (Latora and Marchiori 2001). For a network *N* with *n* nodes and *k* edges, the global efficiency of *N* can be computed as:

$$E_{\text{glob}}^{w}=\frac{1}{n}\sum_{i\in N}\frac{\sum_{j\in N,j\neq i}\left(d_{ij}^{w}\right)^{-1}}{n-1} \quad (3)$$

where d_{ij}^{w} is the shortest path length between node *i* and node *j* in *N*. Global efficiency measures the extent of parallel information transmission at the global network. The local efficiency of G is measured as:

$$E_{loc}^{w}=\frac{1}{n}\sum_{i\in N}E_{\text{glob}}^{w}\left(N_i\right) \quad (4)$$

where $E_{\text{glob}}^{w}\left(N_i\right)$ is the global efficiency of N_i, the subgraph composed of the neighbors of node *i*. Local efficiency quantifies the fault tolerance of the network.

Modularity

Modularity is an important organizational principle for brain networks (Meunier et al. 2010). According to Newman's algorithm (Newman 2004), the modularity index Q^{w} of a weighted network is defined as

$$Q^{w}=\frac{1}{l^{w}}\sum_{i,j\in N}\left[w_{ij}-\frac{k_i^{w}k_j^{w}}{l^{w}}\right]\delta_{m_i,m_j} \quad (5)$$

Where 필w is the sum of all weights in the network, w_{ij} is connection weights between node *i* and node *j*, k_i is the degree of node *i*, i.e., the number of non-zero connections, m_i is the module containing node 핗, and $\delta_{mi,mj}=1$ if $m_i=m_j$, and 0 otherwise. Modularity quantifies the extent of modular organization. The aim of the module identification process is to find a specific partition that yields the largest network modularity, $\tilde{Q}_{\max}$.

To assess the inter- and intra-modular connectivities, we calculated the participation coefficient (PC) and intra-module degree (MD) for each node to detect the inter- and intra-module connection density (Guimera and Amaral 2005). For a weighted network, participation coefficient is defined as:

$$y_i^{w}=1-\sum_{m\in M}\left(\frac{k_i^{w}(m)}{k_i^{w}}\right)^{2} \quad (6)$$

where 필 is the set of modules and $k_i^{w}(m)$ is the weight of links between *i* and all nodes in module *m*. For a weighted network, weighted within-module degree z-score is define

$$z_i^w = \frac{k_i^w(m_i) - \overline{k}^w(m_i)}{\sigma^{k^w(m_i)}} \quad (7)$$

where m_i is the module containing node i, $k_i^w(m_i)$ is the within-module degree of i (the number of links between i and all other nodes in mi), and $\overline{k}^w(m_i)$ and $\sigma^{k^w}(m_i)$ are the respective mean and standard deviation of the within-module m_i degree distribution.

References

Arfken M. Brain, Mind, and Human Behavior in Contemporary Cognitive Science: Critical Assessments of the Philosophy of Psychology. Theory & Psychology. 2009; 19(6):860–862.

Arnemann KL, Chen AJW, Novakovic-Agopian T, Gratton C, Nomura EM, D'Esposito M. Functional brain network modularity predicts response to cognitive training after brain injury. Neurology. 2015; 84(15):1568–1574. [PubMed: 25788557]

Balenzuela P, Chernomoretz A, Fraiman D, Cifre I, Sitges C, Montoya P, et al. Modular organization of brain resting state networks in chronic back pain patients. Front Neuroinform. 2010; 4:116.doi: 10.3389/fninf.2010.00116 [PubMed: 21206760]

Biswal BB, Mennes M, Zuo XN, Gohel S, Kelly C, Smith SM, et al. Toward discovery science of human brain function. Proceeding of the National Academy of Science of the United States of Aamerica. 2010; 107(10):4734–4739.

Blair RJ, Mitchell DG. Psychopathy, attention and emotion. Psychol Med. 2009; 39(4):543–555. [PubMed: 18700991]

Bonelli RM, Cummings JL. Frontal-subcortical circuitry and behavior. Dialogues Clin Neurosci. 2007; 9(2):141–151. [PubMed: 17726913]

Brown D, Larkin F, Sengupta S, Romero-Ureclay JL, Ross CC, Gupta N, et al. Clozapine: an effective treatment for seriously violent and psychopathic men with antisocial personality disorder in a UK high-security hospital. CNS Spectrums. 2014; 19(5):391–402. [PubMed: 24698103]

Buckner RL, Carroll DC. Self-projection and the brain. Trends Cogn Sci. 2007; 11(2):49–57. [PubMed: 17188554]

Bullmore ET, Suckling J, Overmeyer S, Rabe-Hesketh S, Taylor E, Brammer MJ. Global, voxel, and cluster tests, by theory and permutation, for a difference between two groups of structural MR images of the brain. IEEE Trans Med Imaging. 1999; 18(1):32–42. [PubMed: 10193695]

Campbell-Meiklejohn DK, Kanai R, Bahrami B, Bach DR, Dolan RJ, Roepstorff A, et al. Structure of orbitofrontal cortex predicts social influence. Curr Biol. 2012; 22(4):123–124.

Caspers S, Schleicher A, Bacha-Trams M, Palomero-Gallagher N, Amunts K, Zilles K. Organization of the Human Inferior Parietal Lobule Based on receptor architectonics. Cereb Cortex. 2012; 23(3):615–628. [PubMed: 22375016]

Cavanna AE, Trimble MR. The precuneus: a review of its functional anatomy and behavioural correlates. Brain. 2006; 129(Pt 3):564–583. [PubMed: 16399806]

Cole MW, Repovs G, Anticevic A. The frontoparietal control system: a central role in mental health. Neuroscientist. 2014; 20(6):652–664. [PubMed: 24622818]

de Oliveira-Souza R, Hare RD, Bramati IE, Garrido GJ, Ignacio FA, Tovar-Moll F, et al. Psychopathy as a disorder of the moral brain: fronto-temporo-limbic grey matter reductions demonstrated by voxel-based morphometry. NeuroImage. 2008; 40(3):1202–1213. [PubMed: 18289882]

Demeter E, Hernandez-Garcia L, Sarter M, Lustig C. Challenges to attention: a continuous arterial spin labeling (ASL) study of the effects of distraction on sustained attention. NeuroImage. 2011; 54(2): 1518–1529. [PubMed: 20851189]

Dosenbach NU, Nardos B, Cohen AL, Fair DA, Power JD, Church JA, et al. Prediction of individual brain maturity using fMRI. Science. 2010; 329(5997):1358–1361. [PubMed: 20829489]

Fazel S, Danesh J. Serious mental disorder in 23000 prisoners: a systematic review of 62 surveys. Lancet. 2002; 359(9306):545–550. [PubMed: 11867106]

Fecteau S, Pascual-Leone A, Zald DH, Liguori P, Theoret H, Boggio PS, et al. Activation of prefrontal cortex by trans-cranial direct current stimulation reduces appetite for risk during ambiguous decision making. J Neurosci. 2007; 27(23):6212–6218. [PubMed: 17553993]

Fox MD, Zhang D, Snyder AZ, Raichle ME. The global signal and observed anticorrelated resting state brain networks. J Neurophysiol. 2009; 101(6):3270–3283. [PubMed: 19339462]

Gamboa OL, Tagliazucchi E, von Wegner F, Jurcoane A, Wahl M, Laufs H, et al. Working memory performance of early MS patients correlates inversely with modularity increases in resting state functional connectivity networks. NeuroImage. 2014; 94:385–395. [PubMed: 24361662]

Guimera R, Amaral LAN. Functional cartography of complex metabolic networks. Nature. 2005; 433(7028):895–900. [PubMed: 15729348]

Hawkins KM, Sayegh P, Yan X, Crawford JD, Sergio LE. Neural Activity in Superior Parietal Cortex during Rule-based Visual-motor Transformations. J Cogn Neurosci. 2012; 25(3):436–454. [PubMed: 23092356]

Hoppenbrouwers SS, Nazeri A, de Jesus DR, Stirpe T, Felsky D, Schutter DJ, et al. White matter deficits in psychopathic offenders and correlation with factor structure. PLoS One. 2013; 8(8):e72375.doi: 10.1371/journal.pone.0072375 [PubMed: 23977291]

Jastorff J, Clavagnier S, Gergely G, Orban GA. Neural mechanisms of understanding rational actions: middle temporal gyrus activation by contextual violation. Cereb Cortex. 2011; 21(2):318–329. [PubMed: 20513657]

Koenigs M, Barbey AK, Postle BR, Grafman J. Superior parietal cortex is critical for the manipulation of information in working memory. J Neurosci. 2009; 29(47):14980–14986. [PubMed: 19940193]

Kolb, B., Whishaw, I. Fundamentals of human neuropsychology. New York: WH Freeman and Co; 1990.

Kumari V, Uddin S, Premkumar P, Young S, Gudjonsson GH, Raghuvanshi S, et al. Lower anterior cingulate volume in seriously violent men with antisocial personality disorder or schizophrenia and a history of childhood abuse. Aust N Z J Psychiatry. 2014; 48(2):153–161. [PubMed: 24234836]

Latora V, Marchiori M. Efficient behavior of small-world networks. Phys Rev Lett. 2001; 87(19)doi: 10.1103/Physrevlett.87.198701

Latora V, Marchiori M. Economic small-world behavior in weighted networks. European Physical Journal B. 2003; 32(2):249–263.

Liu H, Liao J, Jiang W, Wang W. Changes in low-frequency fluctuations in patients with antisocial personality disorder revealed by resting-state functional MRI. PLoS One. 2014; 9(3)doi: 10.1371/journal.pone.0089790

Lynall ME, Bassett DS, Kerwin R, McKenna PJ, Kitzbichler M, Muller U, et al. Functional connectivity and brain networks in schizophrenia. J Neurosci. 2010; 30(28):9477–9487. [PubMed: 20631176]

Maslov S, Sneppen K. Specificity and stability in topology of protein networks. Science. 2002; 296(5569):910–913. [PubMed: 11988575]

Meshi D, Biele G, Korn CW, Heekeren HR. How expert advice influences decision making. PLoS One. 2012; 7(11)doi: 10.1371/journal.pone.0049748

Meunier D, Lambiotte R, Bullmore ET. Modular and hierarchically modular organization of brain networks. Front Neurosci. 2010; 4:200.doi: 10.3389/fnins.2010.00200 [PubMed: 21151783]

Meyer ML, Masten CL, Ma YN, Wang CB, Shi ZH, Eisenberger NI, et al. Empathy for the social suffering of friends and strangers recruits distinct patterns of brain activation. Soc Cogn Affect Neurosci. 2013; 8(4):446–454. [PubMed: 22355182]

Meyers CA, Berman SA, Scheibel RS, Hayman A. Case-Report - Acquired Antisocial Personality-Disorder Associated with Unilateral Left Orbital Frontal-Lobe Damage. J Psychiatry Neurosci. 1992; 17(3):121–125. [PubMed: 1390621]

Miller BL, Darby A, Benson D, Cummings J, Miller M. Aggressive, socially disruptive and antisocial behaviour associated with fronto-temporal dementia. Br J Psychiatry. 1997; 170(2):150–154. [PubMed: 9093504]

Moffitt TE, Caspi A, Harrington H, Milne BJ. Males on the life-course-persistent and adolescence-limited antisocial pathways: follow-up at age 26 years. Dev Psychopathol. 2002; 14(1):179–207. [PubMed: 11893092]

Moore TL, Schettler SP, Killiany RJ, Rosene DL, Moss MB. Effects on executive function following damage to the pre-frontal cortex in the rhesus monkey. Behav Neurosci. 2009; 123(2):231–241. [PubMed: 19331446]

Muller JL, Ganssbauer S, Sommer M, Dohnel K, Weber T, Schmidt-Wilcke T, et al. Gray matter changes in right superior temporal gyrus in criminal psychopaths. Evidence from voxel-based morphometry. Psychiatry Research-Neuroimaging. 2008a; 163(3):213–222.

Muller JL, Sommer M, Dohnel K, Weber T, Schmidt-Wilcke T, Hajak G. Disturbed prefrontal and temporal brain function during emotion and cognition interaction in criminal psychopathy. ss. 2008b; 26(1):131–150.

Murphy K, Birn RM, Handwerker DA, Jones TB, Bandettini PA. The impact of global signal regression on resting state correlations: are anti-correlated networks introduced? Neuroimage. 2009; 44(3):893–905. [PubMed: 18976716]

Newman ME, Girvan M. Finding and evaluating community structure in networks. Phys Rev E. 2004; 69(2 Pt 2)doi: 10.1103/PhysRevE.69.026113

Newman MEJ. Modularity and community structure in networks. Proc Natl Acad Sci U S A. 2006; 103(23):8577–8582. [PubMed: 16723398]

Ogilvie JM, Stewart AL, Chan RCK, Shum DHK. Neuropsychological measures of executive function and antisocial behavior: A Meta-Analysis. Criminology. 2011; 49(4):1063–1107.

Onnela JP, Saramaki J, Kertesz J, Kaski K. Intensity and coherence of motifs in weighted complex networks. Phys Rev E. 2005; 71(6)doi: 10.1103/Physreve.71.065103

Peng Z, Shi F, Shi C, Yang Q, Chan RC, Shen D. Disrupted cortical network as a vulnerability marker for obsessive-compulsive disorder. Brain Struct Funct. 2014; 219(5):1801–1812. [PubMed: 23797209]

Philippi CL, Pujara MS, Motzkin JC, Newman J, Kiehl KA, Koenigs M. Altered resting-state functional connectivity in cortical networks in psychopathy. J Neurosci. 2015; 35(15):6068–6078. [PubMed: 25878280]

Potegal M. Temporal and frontal lobe initiation and regulation of the top-down escalation of anger and aggression. Behav Brain Res. 2012; 231(2):386–395. [PubMed: 22085875]

Power JD, Cohen AL, Nelson SM, Wig GS, Barnes KA, Church JA, et al. Functional Network Organization of the Human Brain. Neuron. 2011; 72(4):665–678. [PubMed: 22099467]

Radua J, Phillips ML, Russell T, Lawrence N, Marshall N, Kalidindi S, et al. Neural response to specific components of fearful faces in healthy and schizophrenic adults. NeuroImage. 2010; 49(1):939–946. [PubMed: 19699306]

Raine A, Lencz T, Bihrle S, LaCasse L, Colletti P. Reduced prefrontal gray matter volume and reduced autonomic activity in antisocial personality disorder. Arch Gen Psychiatry. 2000; 57(2):119–127. [PubMed: 10665614]

Raine A, Moffitt TE, Caspi A, Loeber R, Stouthamer-Loeber M, Lynam D. Neurocognitive impairments in boys on the life-course persistent antisocial path. J Abnorm Psychol. 2005; 114(1): 38–49. [PubMed: 15709810]

Rascovsky K, Hodges JR, Knopman D, Mendez MF, Kramer JH, Neuhaus J, et al. Sensitivity of revised diagnostic criteria for the behavioural variant of frontotemporal dementia. Brain. 2011; 134(Pt 9):2456–2477. [PubMed: 21810890]

Reichardt J, Bornholdt S. When are networks truly modular? Physica D-Nonlinear Phenomena. 2006; 224(1–2):20–26.

Rubinov M, Sporns O. Complex network measures of brain connectivity: uses and interpretations. NeuroImage. 2010; 52(3):1059–1069. [PubMed: 19819337]

Rubinov M, Sporns O, van Leeuwen C, Breakspear M. Symbiotic relationship between brain structure and dynamics. BMC Neurosci. 2009; 10doi: 10.1186/1471-2202-10-55

Schneider F, Habel U, Kessler C, Posse S, Grodd W, Muller-Gartner HW. Functional imaging of conditioned aversive emotional responses in antisocial personality disorder. Neuropsychobiology. 2000; 42(4):192–201. [PubMed: 11096335]

Seguin JR, Sylvers P, Lilienfeld SO. The Neuropsychology of Violence. Cambridge. Handbook of Violent Behavior and Aggression. 2007:187–214.

Shi F, Wang L, Peng ZW, Wee CY, Shen DG. Altered modular Organization of Structural Cortical Networks in children with autism. PLoS One. 2013; 8(5)doi: 10.1371/journal.pone.0063131

Shi F, Yap PT, Gao W, Lin W, Gilmore JH, Shen D. Altered structural connectivity in neonates at genetic risk for schizophrenia: a combined study using morphological and white matter networks. NeuroImage. 2012; 62(3):1622–1633. [PubMed: 22613620]

Sporns O. The human connectome: a complex network. Year in Cognitive Neuroscience. 2011; 1224:109–125.

Sporns O, Zwi JD. The small world of the cerebral cortex. Neuroinformatics. 2004; 2(2):145–162. [PubMed: 15319512]

Stam CJ. Functional connectivity patterns of human magnetoencephalographic recordings: a 'small-world' network? Neurosci Lett. 2004; 355(1–2):25–28. [PubMed: 14729226]

Sundram F, Deeley Q, Sarkar S, Daly E, Latham R, Craig M, et al. White matter microstructural abnormalities in the frontal lobe of adults with antisocial personality disorder. Cortex. 2012; 48(2): 216–229. [PubMed: 21777912]

Supekar K, Menon V, Rubin D, Musen M, Greicius MD. Network analysis of intrinsic functional brain connectivity in Alzheimer's disease. PLoS Comput Biol. 2008; 4(6):e1000100. [PubMed: 18584043]

Tagliazucchi E, von Wegner F, Morzelewski A, Brodbeck V, Borisov S, Jahnke K, et al. Large-scale brain functional modularity is reflected in slow electroencephalographic rhythms across the human non-rapid eye movement sleep cycle. NeuroImage. 2013; 70:327–339. [PubMed: 23313420]

Talati A, Hirsch J. Functional specialization within the medial frontal gyrus for perceptual go/no-go decisions based on "what," "when," and "where" related information: An fMRI study. J Cogn Neurosci. 2005; 17(7):981–993. [PubMed: 16102231]

Tang Y, Jiang W, Liao J, Wang W, Luo A. Identifying individuals with antisocial personality disorder using resting-state FMRI. PLoS One. 2013; 8(4)doi: 10.1371/journal.pone.0060652

Tzourio-Mazoyer N, Landeau B, Papathanassiou D, Crivello F, Etard O, Delcroix N, et al. Automated anatomical labeling of activations in SPM using a macroscopic anatomical parcellation of the MNI MRI single-subject brain. NeuroImage. 2002; 15(1):273–289. [PubMed: 11771995]

Vaessen MJ, Braakman HMH, Heerink JS, Jansen JFA, Debeij-van Hall MHJA, Hofman PAM, et al. Abnormal modular Organization of Functional Networks in cognitively impaired children with frontal lobe epilepsy. Cereb Cortex. 2013; 23(8):1997–2006. [PubMed: 22772649]

Vincent JL, Kahn I, Snyder AZ, Raichle ME, Buckner RL. Evidence for a frontoparietal control system revealed by intrinsic functional connectivity. J Neurophysiol. 2008; 100(6):3328–3342. [PubMed: 18799601]

Vogt BA, Laureys S. Posterior cingulate, precuneal and retrosplenial cortices: cytology and components of the neural network correlates of consciousness. Prog Brain Res. 2005; 150:205–217. [PubMed: 16186025]

Volz KG, Schubotz RI, von Cramon DY. Uncertainty in decision making and its neural correlates. J Psychophysiol. 2004a; 18(4):201–202.

Volz KG, Schubotz RI, von Cramon DY. Why am I unsure? Internal and external attributions of uncertainty dissociated by fMRI. NeuroImage. 2004b; 21(3):848–857. [PubMed: 15006651]

Walton ME, Behrens TEJ, Buckley MJ, Rudebeck PH, Rushworth MFS. Separable learning Systems in the Macaque Brain and the role of orbitofrontal cortex in contingent learning. Neuron. 2010; 65(6):927–939. [PubMed: 20346766]

Wang J, Zuo X, Dai Z, Xia M, Zhao Z, Zhao X, et al. Disrupted functional brain connectome in individuals at risk for Alzheimer's disease. Biol Psychiatry. 2013; 73(5):472–481. [PubMed: 22537793]

Watts DJ, Strogatz SH. Collective dynamics of 'small-world' networks. Nature. 1998; 393(6684):440–442. [PubMed: 9623998]

Wee CY, Zhao Z, Yap PT, Wu G, Shi F, Price T, et al. Disrupted brain functional network in internet addiction disorder: a resting-state functional magnetic resonance imaging study. PLoS One. 2014; 9(9)doi: 10.1371/journal.pone.0107306

Widiger TA, Costa PT Jr. Personality and personality disorders. J Abnorm Psychol. 1994; 103(1):78–91. [PubMed: 8040485]

Wolf RC, Pujara MS, Motzkin JC, Newman JP, Kiehl KA, Decety J, et al. Interpersonal traits of psychopathy linked to reduced integrity of the uncinate fasciculus. Hum Brain Mapp. 2015; 36(10):4202–4209. [PubMed: 26219745]

Yan C, Zang Y. DPARSF: A MATLAB toolbox for "pipeline" data analysis of resting-state fMRI. Front Syst Neurosci. 2010; 4:13.doi: 10.3389/fnsys.2010.00013 [PubMed: 20577591]

Yang Y, Raine A. Prefrontal structural and functional brain imaging findings in antisocial, violent, and psychopathic individuals: a meta-analysis. Psychiatry Res. 2009; 174(2):81–88. [PubMed: 19833485]

Zahn R, Moll J, Iyengar V, Huey ED, Tierney M, Krueger F, et al. Social conceptual impairments in frontotemporal lobar degeneration with right anterior temporal hypometabolism. Brain. 2009; 132:604–616. [PubMed: 19153155]

Zalesky A, Fornito A, Bullmore ET. Network-based statistic: identifying differences in brain networks. NeuroImage. 2010; 53(4):1197–1207. [PubMed: 20600983]

Zhang J, Wang J, Wu Q, Kuang W, Huang X, He Y, et al. Disrupted brain connectivity networks in drug-naive, first-episode major depressive disorder. Biol Psychiatry. 2011; 70(4):334–342. [PubMed: 21791259]

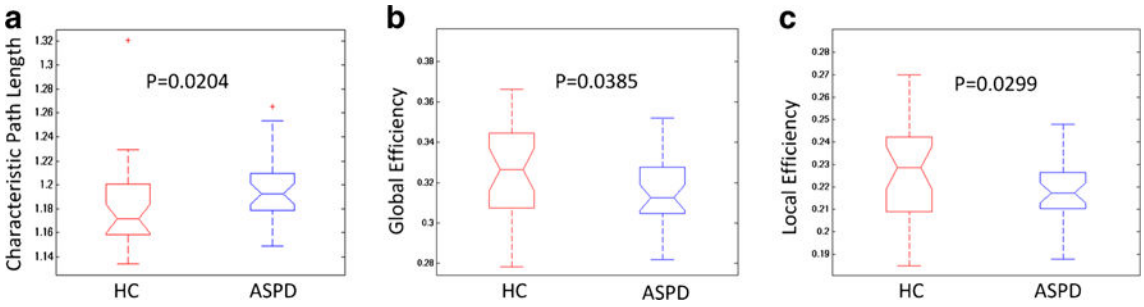

Fig. 1.

Difference of small-world parameters of functional brain networks between ASPD and controls using non-parametric permutation test: (**a**) Functional brain networks exhibited increased characteristic path length. (**b**) Functional brain networks exhibited decreased global network efficiency (Eglob). (**c**) Functional brain networks exhibited decreased local network efficiency (Eloc)

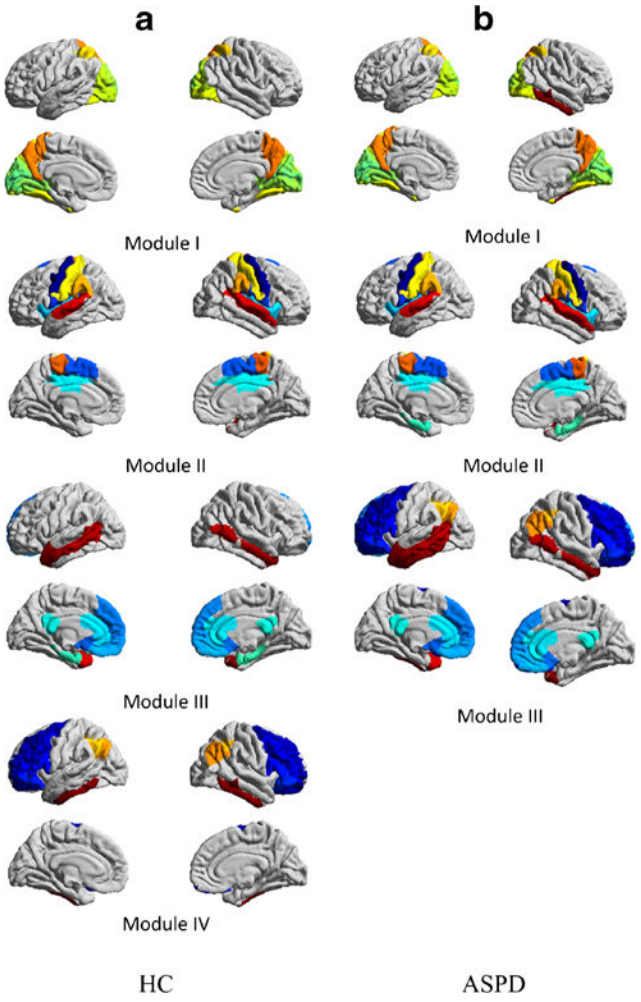

Fig. 2.

Modularity of group-averaged functional connectivity networks: (**a**) Modular membership of healthy controls. Module I: Posterior; Module II: Central; Module III: Frontal-Subcortical; Module IV: Frontoparietal. (**b**) Modular membership of ASPD patients. Module I: Posterior; Module II: Central; Module III: Frontal-Subcortical; Module IV: Fronto-Parietal-Subcortical

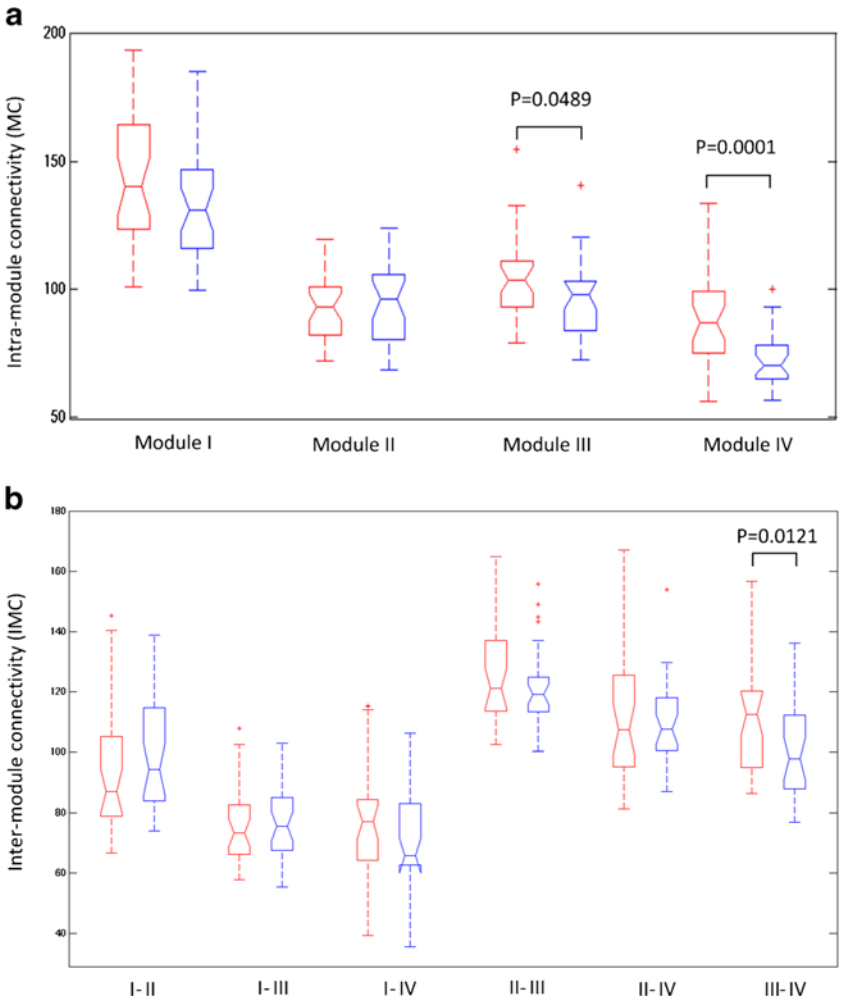

Fig. 3.

Module connectivity analysis using non-parametric permutation test: (**a**) Between-group difference in the intra-module connectivity. (**b**) Between-group difference in the inter-module connectivity. Module I: Posterior; Module II: Central module; Module III: Frontal-Subcortical; Module IV: Frontoparietal. Red represents HC, blue represents ASPD

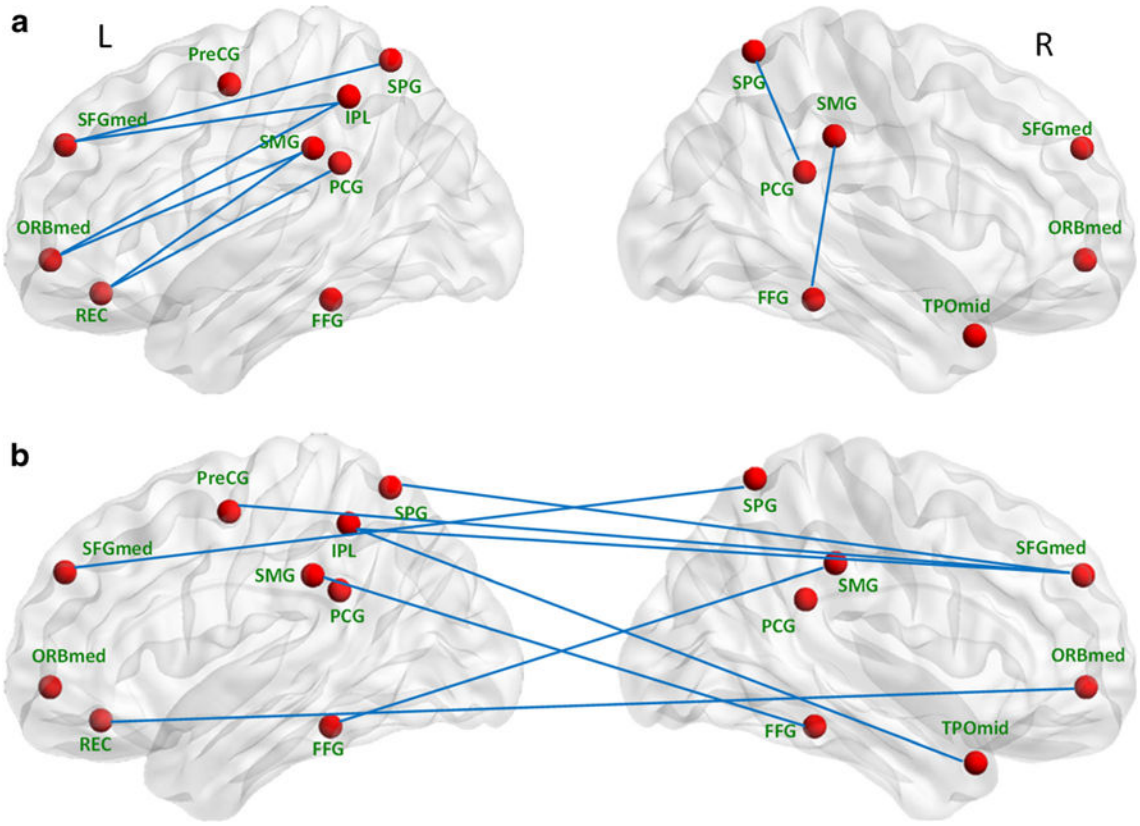

Fig. 4.

The altered functional connectivities in ASPD patients in comparison to normal controls, based on network statistics. (**a**) Decreased functional connectivities within left or right hemisphere. (**b**) Decreased functional connectivities between left and right hemispheres. L: left, R: right

Table 1

Characteristics of the participants in this study

	ASPD (Mean ± SD)	**Controls (Mean ± SD)**	***P* value**
Number	32	35	–
Gender	32 males	35 males	–
Age (Years)	20.5 ± 1.37	21.67 ± 2.54	0.8551
Education(Years)	8.32 ± 1.54	9.73 ± 0.82	0.7526
IQ	106.66 ± 12.90	106.84 ± 16.6	0.7733

ASPD: Offenders with antisocial personality disorder

Table 2

Altered brain regions in modularity analysis of antisocial personality disorder using nonparametric permutation test

Brain Region	Abbreviation	t-value	*p*-value
Participation coefficient			
Orbitofrontal cortex (middle) right	ORBmid-R	−2.7050	0.0090
Orbitofrontal cortex (inferior) left	ORBinf-L	−2.1805	0.0334
Supplementary motor area left	SMA-L	−2.2997	0.0252
Rolandic operculum right	ROL-R	−2.1114	0.0391
Superior frontal gyrus (medial) left	SFGmed-L	−2.7502	0.0080
Superior frontal gyrus (medial) right	SFGmed-R	−2.2472	0.0285
Insula right	INS-R	−2.3877	0.0203
Posterior cingulate gyrus left	PCG-L	2.1525	0.0356
Superior occipital gyrus left	SOG-L	−2.7428	0.0081
Superior occipital gyrus right	SOG-R	−2.1902	0.0326
Postcentral gyrus right	PoCG-R	−2.4306	0.0182
Superior parietal gyrus left	SPG-L	−3.0220	0.0038
Superior parietal gyrus right	SPG-R	−3.6426	0.0006
Inferior parietal lobule left	IPL-L	−3.8170	0.0003
Inferior parietal lobule right	IPL-R	−2.2846	0.0261
Supramarginal gyrus left	SMG-L	−2.7190	0.0087
Supramarginal gyrus right	SMG-R	−3.0413	0.0036
Heschl gyrus left	HES-L	−2.1870	0.0329
Heschl gyrus right	HES-R	−2.3587	0.0218
Superior temporal gyrus left	STG-L	−2.1230	0.0381
Module degree			
Inferior frontal gyrus (opercular) right	IFGoperc-R	−3.1126	0.0029
Rolandic operculum right	ROL-R	−2.4765	0.0163
Superior frontal gyrus (medial) left	SFGmed-L	2.8059	0.0069
Superior frontal gyrus (medial) right	SFGmed-R	2.1954	0.0322
Posterior cingulate gyrus left	PCG-L	−3.3318	0.0015
Posterior cingulate gyrus right	PCG-R	−3.3661	0.0014
Hippocampus right	HIP-R	−2.0638	0.0436
Lingual gyrus right	LING-R	−2.7971	0.0070
Superior occipital gyrus left	SOG-L	2.2815	0.0263
nferior occipital gyrus right	IOG-R	−2.0928	0.0408
Superior parietal gyrus left	SPG-L	2.8189	0.0066
Temporal pole (superior) left	TPOsup-L	3.9701	0.0002
Middle temporal gyrus left	MTG-L	2.8894	0.0054
Inferior temporal gyrus left	ITG-L	3.2007	0.0022
Inferior temporal gyrus right	ITG-R	2.2912	0.0257

Participation coefficient: PC, a measure of diversity of intermodular connections of individual nodes;
Module degree: MD, a within-module version of degree centrality